Conditions for anti-Zeno effect observation in free-space atomic radiative decay

Emmanuel Lassalle, Caroline Champenois, Brian Stout, Vincent Debierre, Thomas Durt

Conditions for anti-Zeno effect observation in free-space atomic radiative decay

Emmanuel Lassalle,[1] Caroline Champenois,[2] Brian Stout,[1] Vincent Debierre,[3,*] and Thomas Durt[1]

[1] *Aix Marseille Université, CNRS, Centrale Marseille, Institut Fresnel UMR 7249, 13013 Marseille, France*
[2] *Aix Marseille Université, CNRS, PIIM UMR 7345, 13013 Marseille, France*
[3] *Max Planck Institute for Nuclear Physics, Saupfercheckweg 1, 69117 Heidelberg, Germany*

(Dated: June 12, 2018)

Frequent measurements can modify the decay of an unstable quantum state with respect to the free dynamics given by Fermi's golden rule. In a landmark article, *Nature* **405**, 546 (2000), Kofman and Kurizki concluded that in quantum decay processes, acceleration of the decay by frequent measurements, called the quantum anti-Zeno effect (AZE), appears to be ubiquitous, while its counterpart, the quantum Zeno effect, is unattainable. However, up to now there have been no experimental observations of the AZE for atomic radiative decay (spontaneous emission) in free space. In this work, making use of analytical results available for hydrogen-like atoms, we find that in free space, only non-electric-dipolar transitions should present an observable AZE, revealing that this effect is consequently much less ubiquitous than first predicted. We then propose an experimental scheme for AZE observation, involving the electric quadrupole transition between $D_{5/2}$ and $S_{1/2}$ in the alkali-earth ions Ca^+ and Sr^+. The proposed protocol is based on the STIRAP technique which acts like a dephasing quasi-measurement.

I. INTRODUCTION

One of the more peculiar features of quantum mechanics is that the measurement process can modify the evolution of a quantum system. The archetypes of this phenomenon are the quantum Zeno effect (QZE) and the quantum anti-Zeno effect (AZE) [1, 2]. The QZE refers to the inhibition of the decay of an unstable quantum system due to frequent measurements [3], and was observed experimentally for the first time with trapped ions [4, 5] and more recently in cold neutral atoms [6]. The opposite effect, where the decay is *accelerated* by frequent measurements, was first called the AZE in Ref. [7], and was discovered theoretically for spontaneous emission in cavities [8, 9], and first observed in a tunneling experiment with cold atoms (along with the QZE) [10], and recently with a single superconducting qubit coupled to a waveguide cavity [11]. However, despite predictions that the AZE should be much more ubiquitous than the QZE in radiative decay processes [1], it has never been observed to our knowledge for atomic radiative decay (spontaneous emission) in free space.

Here, we investigate the case of hydrogen-like atoms, for which the exact expression of the coupling between the atom and the free radiative field (*cf.* [12, 13]) allows us to derive an analytical expression for the measurement-modified decay rate. From this, we find that only non-electric-dipole transitions can exhibit the AZE in free space (*i.e.* non-dipole electric transitions *and* magnetic transitions of *any* multipolar order), which drastically limits the experimental possibilities to observe this effect. We start with a brief review of the general formal results about the measurement-modified decay rate in Sec. II, and we then apply, in Sec. III, this general framework to the case of electronic transitions in hydrogen-like atoms to derive an analytical expression of the measurement-modified decay rate in free space. Then, we discuss the experimental realizability of the described phenomenon in Sec. IV, and we identify a potential candidate: the electric quadrupole transition between $D_{5/2}$ and $S_{1/2}$ in Ca^+ or Sr^+. Conclusions are finally given in Sec. V.

II. MONITORED SPONTANEOUS EMISSION: GENERAL ANALYSIS

We consider a two-level atom in free space, consisting of a ground state $|g\rangle$ and an excited state $|e\rangle$ separated by the Bohr energy $\hbar\omega_0$, and initially prepared in $|e\rangle$. Due to the coupling with the modes of the electromagnetic (EM) reservoir, the atom will naturally decay to the ground state $|g\rangle$, with a survival probability to stay in the excited state $|e\rangle$ given by $P(t) = \exp(-\Gamma t)$ (Wigner-Weisskopf decay [14]). For the free dynamics (*i.e.* without measurements), the decay rate Γ is given by the Fermi's golden rule (FGR) [14], and will be denoted by Γ_0 in the following.

In Ref. [1], Kofman and Kurizki showed that frequent measurements on an excited two-level atom, *i.e.* repeated instantaneous projections onto the state $|e\rangle$, lead to a broadening of its energy level, analogous to collisional broadening. Therefore, the atom probes a larger range of EM modes in the reservoir spectrum, and these new decay channels might modify the dynamics. Specifically, it was shown, within the rotating-wave approximation (RWA), that if frequent measurements are performed at short intervals τ, the dynamics still follows an exponential decay, but with a measurement-modified decay rate given by [1]

$$\Gamma = 2\pi \int_0^\infty \mathrm{d}\omega \, F_\tau \left(\omega - \omega_0\right) R\left(\omega\right) \ . \tag{1}$$

The effects of the RWA on the QZE and AZE have been

* vincent.debierre@mpi-hd.mpg.de

discussed in Refs. [15, 16], showing no essential differences between the predictions made with and without the RWA in the case of the reservoir that we shall consider here. Moreover, for a discussion about a non-exponential decay, see Ref. [17].

In Eq. (1), the function $R(\omega)$ represents the reservoir coupling spectrum and is written

$$R(\omega) = \hbar^{-2} \sum_k |\langle \mathrm{e}, 0| \hat{H}_I |\mathrm{g}, 1_k\rangle|^2 \delta(\omega - \omega_k) \qquad (2)$$

where $|\mathrm{g}, 1_k\rangle = |\mathrm{g}\rangle \otimes |1_k\rangle$ is the outer product between the atomic state $|\mathrm{g}\rangle$ and the state of the EM field $|1_k\rangle$ containing one photon in the mode labelled by k, $|\mathrm{e}, 0\rangle = |\mathrm{e}\rangle \otimes |0\rangle$ is the outer product between the atomic state $|\mathrm{e}\rangle$ and the vacuum state of the EM field $|0\rangle$, and $\hat{H}_I$ is the interaction Hamiltonian. The function $F_\tau(\omega - \omega_0)$, on the other hand, corresponds to the broadened spectral profile of the atom due to the frequent measurements at a rate $\nu = 1/\tau$, and takes the form

$$F_\tau(\omega - \omega_0) = \frac{\tau}{2\pi} \mathrm{sinc}^2\left((\omega - \omega_0)\frac{\tau}{2}\right) \qquad (3)$$

with $\mathrm{sinc}(x) \equiv \sin(x)/x$. Note that the spectral profile function can be generalized to the case where no assumption is made beforehand about the state that is being repeatedly prepared [18]. In Fig. 1 (a) (orange line), the function $F_\tau(\omega - \omega_0)$ is shown, centered on ω_0 and with a width of about $2\pi\nu$. When $\nu \to 0$, $F_\tau(\omega - \omega_0) \to \delta(\omega - \omega_0)$ and Eq. (1) gives: $\Gamma \to 2\pi R(\omega_0)$, which is the natural decay rate given by the FGR $\Gamma_0 \equiv 2\pi R(\omega_0)$, where only the single photon states of frequency ω_0 contribute to the decay.

From Eq. (1), we can see that the measurement-modified decay rate corresponds to the overlap between the functions $R(\omega)$ and $F_\tau(\omega - \omega_0)$, and therefore depending on the profile of $R(\omega)$ in the interval around ω_0, the system may experience an acceleration ($\Gamma > \Gamma_0$, AZE) or a deceleration ($\Gamma < \Gamma_0$, QZE) of the decay compared to the measurement-free decay. In the following, we aim at investigating the case of hydrogen-like atoms coupled to the free space EM field, for which the function $R(\omega)$ can be calculated analytically. This will allow us to highlight the conditions for an AZE observation in such systems. Before doing so, however, it is worth mentionning that in the perturbative treatment that we use, Eqs. (1) and (2) are valid to the first order (*i.e.* only one-photon processes are considered), and do not include higher-order contributions (*i.e.* two-photon and many-photon processes). For this approximation to be valid, we need to ensure that, compared to the spontaneous single-photon emission of the $|\mathrm{e}\rangle \to |\mathrm{g}\rangle$ transition considered, two-photon processes, which involve other atomic levels, are negligible. This can only be checked on a case-by-case basis for specific atoms. In Sec. IV, we consider the specific case of the electric quadrupole transition of Ca^+, and we check that the single-photon emission is the dominant decay channel from the relevant excited state (in Sec. IV A).

III. QUANTUM ANTI-ZENO EFFECT IN HYDROGEN-LIKE ATOMS

A. Reservoir coupling spectrum for hydrogen-like atoms

For hydrogen-like atoms, it is useful to write the states of the atom in terms of the multipolar modes $|\mathrm{g}\rangle = |n_\mathrm{g}, l_\mathrm{g}, m_\mathrm{g}\rangle$ and $|\mathrm{e}\rangle = |n_\mathrm{e}, l_\mathrm{e}, m_\mathrm{e}\rangle$ where each atomic state is described by three discrete quantum numbers n_i, l_i and m_i which are respectively the principal, angular momentum and magnetic quantum numbers. Similarly, it is useful to write the one-photon states in the energy-angular-momentum basis [12, 13] $|1_k\rangle = |J, M, \lambda, \omega\rangle$, where a photon is characterized by its angular momentum and magnetic quantum numbers J and M, respectively, and also its helicity λ and frequency ω. Based on the exact calculations of the matrix elements in (non-relativistic) hydrogen-like atoms in *free space* (initiated by Moses [12] and completed by Seke [13]), the reservoir (2) can be obtained analytically and depends on the type of the multipole transition $|\mathrm{e}\rangle \to |\mathrm{g}\rangle$ considered (see Appendix A for details)

$$R(\omega) = \sum_{J=|l_\mathrm{e}-l_\mathrm{g}|}^{|l_\mathrm{e}+l_\mathrm{g}|} \sum_{r=0}^{N_J} \frac{D_{Jr}}{\omega_\mathrm{X}^{\eta_J+2r-1}} \frac{\omega^{\eta_J+2r}}{\left[1 + \left(\frac{\omega}{\omega_\mathrm{X}}\right)^2\right]^\mu} \qquad (4)$$

where $\eta_J = 1 + 2J$ for magnetic transitions, and $\eta_J = -1 + 2J$ for electric transitions with J starts at 1 for a dipole transition ($l_\mathrm{e} - l_\mathrm{g} = 1$), at 2 for a quadrupole transition ($l_\mathrm{e} - l_\mathrm{g} = 2$) and so on; $\mu = 2(n_\mathrm{g} + n_\mathrm{e} - 1)$; D_{Jr} are dimensionless constants involving the Clebsch-Gordan coefficients of the transition under consideration; and ω_X is the non-relativistic cutoff frequency that emerges naturally from calculations [19, 20] and reads [13]:

$$\omega_\mathrm{X} = \left(\frac{1}{n_\mathrm{g}} + \frac{1}{n_\mathrm{e}}\right) \frac{c}{a_0} Z \qquad (5)$$

with a_0 the Bohr radius and Z the atomic number. Finally, the index at which the sum is terminated is $N_J = 2(n_\mathrm{e} + n_\mathrm{g}) - 4 - J - l_\mathrm{e} - l_\mathrm{g} - \epsilon$ with $\epsilon = 0$ for electric transitions and $\epsilon = 1$ for magnetic transitions.

For simplicity, we first consider electric transitions ($\epsilon = 0$) between an excited state of maximal angular momentum ($l_\mathrm{e} = n_\mathrm{e} - 1$) and the ground state $1S$ ($n_\mathrm{g} = 1$, $l_\mathrm{g} = 0$). In that case, $N_J = 0$ and the two sums disappear in Eq. (4) which reduces to

$$R(\omega) = \frac{D}{\omega_\mathrm{X}^{\eta-1}} \frac{\omega^\eta}{\left[1 + \left(\frac{\omega}{\omega_\mathrm{X}}\right)^2\right]^\mu} \qquad (6)$$

where we defined $D \equiv D_{J0}$ and $\eta \equiv \eta_J$. This reservoir coupling spectrum is sketched on Fig. 1 (a). The parameters η, μ and ω_X corresponding to the electric transitions $2P$-$1S$ (dipole), $3D$-$1S$ (quadrupole) or $4F$-$1S$ (octupole) are given in Table I.

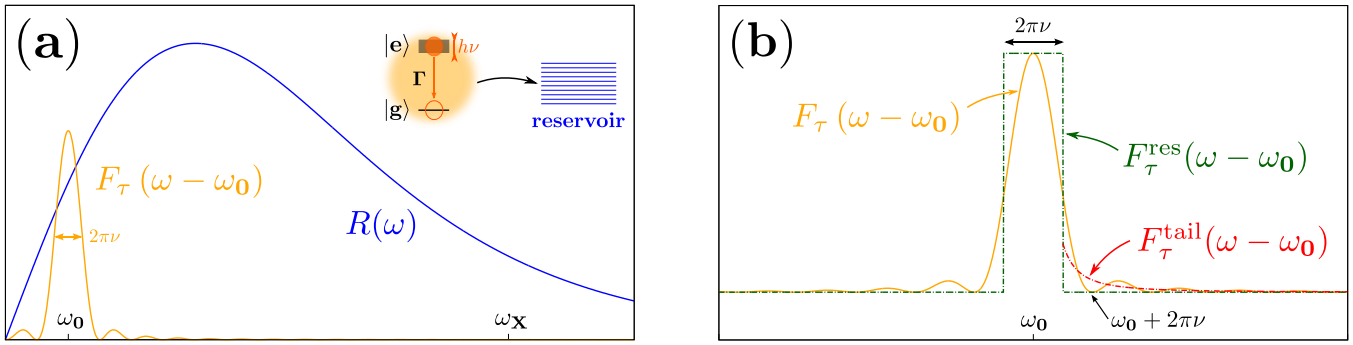

FIG. 1. (a) Scheme of the broadened spectral profile $F_\tau(\omega-\omega_0)$ (orange line) of an atom with transition frequency ω_0 due to repeated measurements at a rate $\nu=1/\tau$ with τ the interval between each measurement, and reservoir coupling spectrum $R(\omega)$ (blue line) of the form of Eq. (6) with a cutoff frequency $\omega_X \gg \omega_0$. (b) Scheme of the broadened spectral profile $F_\tau(\omega-\omega_0)$ (orange line) and its resonant $[F_\tau^{res}(\omega-\omega_0)=1/(2\pi\nu)$ for $-\pi\nu<\omega-\omega_0<\pi\nu$ (green dashed line)] and tail $[F_\tau^{tail}(\omega-\omega_0)=\nu/[\pi(\omega-\omega_0)^2]$ for $\omega-\omega_0>\pi\nu$ (red dashed line)] approximations. The inset shows that the energy broadening of $|e\rangle$, induced by the frequent measurements at rate ν, modifies the decay into the EM reservoir.

Transitions	$2P$-$1S$	$3D$-$1S$	$4F$-$1S$
η	1	3	5
μ	4	6	8
ω_X/ω_0	548.1	411.1	365.4

TABLE I. Parameters of the reservoir spectrum given by Eq. (6) for the electric transitions $2P$-$1S$ (dipole), $3D$-$1S$ (quadrupole) or $4F$-$1S$ (octupole) in the hydrogen atom.

B. Analytical results for $\omega_0 \ll \omega_X$

In this section, we want to derive an analytical expression of the decay rate (1) to see how it scales with the measurement rate ν when the reservoir coupling spectrum is of the form of Eq. (6), in the case $\omega_0 \ll \omega_X$ which is always respected for low-Z atoms. Indeed, using the Bohr formula for ω_0, the ratio between ω_0 and the cutoff frequency ω_X can be written from Eq. (5) as

$$\frac{\omega_0}{\omega_X}=\frac{1}{2}(Z\alpha)\left(\frac{1}{n_g}-\frac{1}{n_e}\right), \tag{7}$$

with α the fine structure constant of electrodynamics of approximate value $\alpha\simeq 1/137$, whence we can see that the assumption $\omega_0 \ll \omega_X$ makes sense for atoms with Z moderately small.

The details of our derivation are given in Appendix B, and we present the main ideas here. In the integral Γ (Eq. (1)), we start by expanding (to all orders) the numerator ω^η of the reservoir function $R(\omega)$ (Eq. (6)) around the transition frequency ω_0. This binomial expansion yields a series of terms of the type $(\omega-\omega_0)^k$ with k integers between 0 and η. We can then consider that the total decay rate in Eq. (1) results from two contributions. (i) A 'resonant' contribution Γ^{res} coming from the $k=0$ and $k=1$ terms of the binomial expansion of ω^η, for which only the part of $F_\tau(\omega-\omega_0)$ that probes the reservoir $R(\omega)$ in a frequency range of width $\sim\nu$ around ω_0 contributes. This amounts to making the approximation that $F_\tau(\omega-\omega_0)=1/(2\pi\nu)$ in the interval $-\pi\nu<\omega-\omega_0<\pi\nu$ and vanishes elsewhere. With the hierarchy $\omega_0 \ll \omega_X$ in mind, the resonant contribution can then be calculated (see Appendix B)

$$\Gamma^{res}\simeq 2\pi\frac{D}{\omega_X^{\eta-1}}\omega_0^\eta \tag{8}$$

and is found to be equal to the natural decay rate $\Gamma_0=2\pi R(\omega_0)\simeq 2\pi D\omega_0^\eta/\omega_X^{\eta-1}$ computed by the FGR. (ii) The 'tail' contribution Γ^{tail}, which only exists if $\eta>1$, comes from all the terms with order $1<k\leq\eta$, for which $F_\tau^{tail}(\omega-\omega_0)\propto 1/(\omega-\omega_0)^2$ probes the entire reservoir and has a non-negligible contribution. By approximating the square sine by its mean value 1/2, we can then compute the tail contribution (see Appendix B)

$$\Gamma^{tail}\simeq D\,\nu\,B\left(\frac{1-\eta}{2}+\mu,-\frac{1-\eta}{2}\right) \tag{9}$$

where B refers to Euler's Beta function and is a simple numerical prefactor (roughly of the order of unity). Finally, the measurement-modified decay rate $\Gamma=\Gamma^{res}+\Gamma^{tail}$ normalized by the natural decay rate Γ_0 yields the result (partially obtained in Ref. [1]):

$$\frac{\Gamma}{\Gamma_0}\simeq\begin{cases}1 \text{ for } \eta=1,\\ 1+\frac{1}{2\pi}\frac{\nu}{\omega_0}\left(\frac{\omega_X}{\omega_0}\right)^{\eta-1}B\left(\frac{1-\eta}{2}+\mu,-\frac{1-\eta}{2}\right)\\ \qquad\qquad \text{for } \eta>1.\end{cases} \tag{10}$$

In Appendix C, we show how this expression can be extended to the general form of $R(\omega)$ given by Eq. (4): the result is similar in terms of scaling with the different parameters η, ν, ω_0 and ω_X; and the Beta function is simply replaced by a more complex numerical prefactor (see Eq. (C3)).

C. Comparison between numerical and analytical calculations and discussion

Before commenting on the scope of this result, we first compare in Fig. 2 the analytical approximation of Γ given by Eq. (10) to the numerical computation $\Gamma^{\rm num}$ of Eq. (1) (using (3) and (6)) for three different reservoir coupling spectra $R(\omega)$ corresponding to the electric dipole ($\eta = 1$, in green), quadrupole ($\eta = 3$, in red) and octupole ($\eta = 5$, in blue) transitions whose parameters are given in Table I. We can see a very good agreement for the quadrupole and octupole transitions up to $\nu \lesssim 100\,\omega_0$, and for the dipolar transition up to $\nu \lesssim \omega_0$. Note that in practice, it may not be feasible to reach such high measurement rates as $\nu \sim \omega_0$ (particularly for optical transitions, *cf.* Sec. IV), and moreover, for $\nu \gtrsim \omega_0$, the RWA is not valid anymore. Therefore, the analytical results are revealed to be excellent in the regime of interest $\nu \ll \omega_0$ with a relative error $(\Gamma^{\rm num} - \Gamma)/\Gamma^{\rm num}$ less than 2% for $\nu/\omega_0 < 10^{-2}$ in the three cases represented on the plot.

Concerning the AZE, we can see that in the case of the electric dipole transition, the AZE trend ($\Gamma > \Gamma_0$) appears only for $\nu \gtrsim \omega_0$ (green curve) — which is not interesting for experimental observations as just discussed, whereas for the other transitions (red and blue curves), the AZE is obtained already for $\nu \ll \omega_0$ and can be very strong. This has been overlooked in the past and constitutes our main result: within the natural hierarchy $\omega_0 \ll \omega_{\rm X}$, we predict from our general Eq. (10) that electric dipole transitions ($\eta = 1$) will *not* exhibit the AZE, whereas the AZE can be expected for all other types of electronic transitions ($\eta > 1$). On the one hand, as electric dipole transitions are arguably the most standard and studied type of electronic transitions in atoms, these predictions make the AZE much less ubiquitous than what had been stated in Ref. [1]. On the other hand, we see from Eq. (10) that for all other transitions, the ratio $\omega_{\rm X}/\omega_0 \gg 1$ may give rise, despite the ratio $\nu/\omega_0 \ll 1$, to a strong anti-Zeno effect $\Gamma \gg \Gamma_0$, particularly for high-order multipolar transitions. The goal of the next section is to identify realistic systems suitable for an AZE observation.

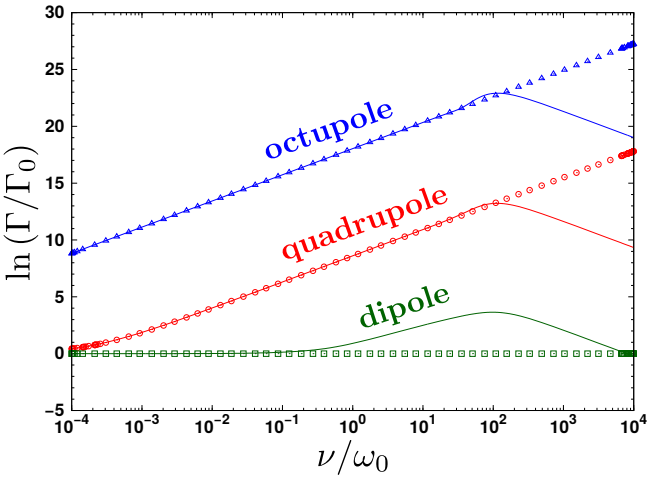

FIG. 2. Comparison between numerical (full lines) and analytical (dotted lines) calculations of $\ln(\Gamma/\Gamma_0)$ as a function of the normalized measurement rate ν/ω_0 for three different electric transitions: dipole ($\eta = 1$, in green), quadrupole ($\eta = 3$, in red) and octupole ($\eta = 5$, in blue). The associated parameters used for the function $R(\omega)$ corresponding to these transitions are displayed in Table I.

IV. EXPERIMENTAL PROPOSAL

A. Transition choice

The search for a possible candidate to observe the AZE is framed by experimental constraints. Even if the AZE is expected to be observable on magnetic dipolar transitions and even more effective on electric octupolar transitions, the very long natural lifetime (of the order of one year or more) of the excited states involved in these transitions makes them very inappropriate to lifetime measurement. Therefore, in what follows, we focus on demonstrating the AZE on an electric quadrupolar transition.

The first choice candidate to confirm the predictions derived for hydrogenic atoms is the hydrogen atom itself, by transferring the atomic population to the lowest D-state (the $3D$-state would play the role of the excited state $|e\rangle$), and frequently monitoring the excited state. A major limit lies in the level scheme of hydrogen which allows an atom in the $3D$-state to decay to the $2P$-states by a strong dipolar transition. The lifetime of the $3D$-state is then conditioned by its dipolar coupling to $2P$ and is not limited by its quadrupolar coupling to $1S$. Therefore, no measurable reduction of the lifetime due to the AZE is expected. The same problem arises with Rydberg states, which were originally proposed as promising candidates [1] for AZE observation due to their transitions in the microwave domain that favor the scaling in $(1/\omega_0)^\eta$ of Eq. (10) compared to optical frequencies.

To circumvent this problem of unwanted transitions, it is then essential to identify a metastable D-state, which has no other decay route to the ground state than the quadrupolar transition. This can be found in the alkali-earth ions like Ca^+ or Sr^+, where the lowest D level is lower in energy than any P-level. The order of magnitude of the lifetime of these D-levels ranges from 1 ms to 1 s. The contribution to the D-level spontaneous emission rate of *two-photon* decay, allowed by second-order perturbation theory based on non-resonant electric-dipole transitions, has been calculated in [21, 22] for Ca^+ and Sr^+. The results show that the two-photon decay channel contributes to 0.01% to the lifetime of the lowest D-states of Ca^+ and Sr^+. As a consequence, the spontaneous emission from the lowest D-level in Ca^+ and Sr^+ can be considered to be due only to electric quadrupolar transition and we then focus on these two atomic systems in the following.

B. Measurement scheme and read-out

Concerning the measurements of the frequently monitored excited state, ideal instantaneous projections on $|e\rangle$ are not strictly required. Indeed, they amount in effect to dephasing the level $|e\rangle$, that is, make the phase of state $|e\rangle$ completely random [1]. Different schemes were proposed to emulate projective measurements in Refs. [1, 23, 24] and performed in Ref. [11], for which Eq. (1) still holds. Here, we propose an alternative protocol in the same spirit of the "dephasing-only measurement" of Ref. [11]. In this scheme, state $|e\rangle$ is the metastable state $D_{5/2}$ and the dephasing measurement is driven by the transition from $D_{5/2}$ to $D_{3/2}$, by two lasers through the strong electric dipolar transitions to the common excited state $P_{3/2}$ (see Fig. 3) using a stimulated Raman adiabatic passage (STIRAP) process [25]. If the two-photon Raman condition is fulfilled (identical detuning for the two transitions), the intermediate $P_{3/2}$-state is not populated and the population is trapped in a coherent superposition of the two states $D_{5/2}$ and $D_{3/2}$. By changing the laser power on each transition with appropriate time profile and time delay, the atomic population can be transferred between the two metastable D-states, like demonstrated in Ref. [26]. After one transfer and return, state $|e\rangle$ thus acquires a phase related to the phase of the two lasers. By applying a random phase jump on one laser between each completed STIRAP transfer, the phase coherence of the excited state $|e\rangle$ is washed out, and a "dephasing" measurement of the level $|e\rangle$ is performed.

To measure the effective lifetime of the $D_{5/2}$-state, the read-out of the internal state must be based on electronic states which do not interfere with $D_{5/2}$. For that purpose, the electron-shelving scheme first proposed by Dehmelt can be used [27]. It requires two other lasers, coupling to the $S_{1/2} \rightarrow P_{1/2}$ and to the $D_{3/2} \rightarrow P_{1/2}$ transitions (see Fig. 3). When shining these two lasers simultaneously, the observation of scattered photons at the $S_{1/2} \rightarrow P_{1/2}$ transition frequency is the signature of the decay of the atom to the ground state [28]. This read-out scheme is switched on during a short time compared to the lifetime of the $D_{5/2}$-state, at a time when the STIRAP process has brought back the electron to $D_{5/2}$.

C. Calculation for $^{40}Ca^+$

We now try to see whether the AZE might be observable in Ca^+, which is not strictly speaking hydrogenic, but is alkali-like in a sense that it has a single valence electron, and can be seen as a single electron orbiting around a core with a net charge $+2e$. Ca^+ is the lightest of the alkali-earth ions having the appropriate level-scheme required for the proposed experimental protocol (see Fig. 3). Therefore, we assume that it still makes sense to use Eq. (10) (derived for hydrogen-like atoms) and we apply it to the electric quadrupole ($\eta = 3$) transition $3D_{5/2} \rightarrow 4S_{1/2}$ to find

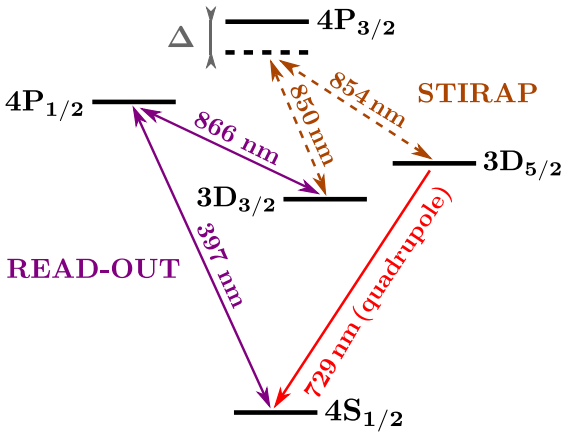

FIG. 3. Dephasing measurement and read-out schemes for AZE observation in $^{40}Ca^+$. The transition used for the AZE is the electric quadrupole transition at 729 nm (red solid arrow). The dephasing measurement can be performed using a STIRAP process between the $D_{5/2}$ and $D_{3/2}$ states *via* two strong electric dipole transitions $D_{5/2} \rightarrow P_{3/2}$ at 854 nm and $D_{3/2} \rightarrow P_{3/2}$ at 850 nm, both detuned from resonance (brown dashed arrows) [26]. The read-out consists in observation of laser induced fluorescence if the atom has decayed to the ground state [27] (purple solid arrows).

$$\frac{\Gamma - \Gamma_0}{\Gamma_0} = A \frac{\nu}{\omega_0} \left(\frac{\omega_X}{\omega_0} \right)^2 \tag{11}$$

where the numerical pre-factor A cannot be computed for such an electronic system (see Appendix C for a calculation of A in the simpler case of hydrogen-like atoms).

To be observable, the AZE must induce a lifetime reduction larger than 1%, the best precision reached in recent $3D_{5/2}$-lifetime measurements in Ca^+ [28]. We evaluate ω_X using Eq. (5) with $n_g = 4$ and $n_e = 3$ and by replacing the atomic number Z by the effective number of charges $Z_{eff} = 2$. Using the frequency of this transition $\omega_0 = 2\pi \times 411$ THz, this gives a ratio $(\omega_X/\omega_0)^2 \simeq 6.6 \cdot 10^6$. If the unknown pre-factor A is assumed to be of the order of unity, one would need $\nu \sim 4$ MHz to meet the observation requirement.

The transfer between the states $D_{5/2}$ and $D_{3/2}$ has been demonstrated in $^{40}Ca^+$ with a STIRAP process [26], where a complete one-way transfer duration of 5 μs was observed for 420 mW/mm^2 on the 850 nm $3D_{3/2} \rightarrow 4P_{3/2}$ transition and 640 mW/mm^2 on the 854 nm $3D_{5/2} \rightarrow 4P_{3/2}$ transition, with both lasers detuned by $\Delta = 600$ MHz from resonance (see Fig. 3). To reduce the duration of the dephasing measurement to time scale smaller than 1 μs, one can increase the laser intensity by stronger focusing and/or larger power, but we can also consider that a complete STIRAP transfer is not required to achieve a dephasing of the excited state. Furthermore, a close inspection of Tables I and II in Ref. [13] suggests that the pre-factor A could be much larger than unity, making the constraint on a high measurement rate less stringent for AZE observation.

Even if the experimental requirements for AZE observation on quadrupole transition in Ca^+ are more demanding than today's best achievements, realistic arguments show that they can be met in a dedicated experimental set-up. This experimental challenge would benefit from theoretical insight concerning the still unknown pre-factor scaling the lifetime reduction.

V. CONCLUSION

Based on well-established results for hydrogen-like atoms, we derived an analytical expression of the decay rate modified by frequent measurements which allows us to highlight the main condition for an observable AZE in atomic radiative decay in free space: all transitions except electric-dipole transitions will exhibit an AZE under sufficiently rapid repeated measurements. This analytical formula also indicates how the AZE scales with the measurement rate. We then identified a suitable level scheme in the alkali-earth ions Ca^+ and Sr^+ for AZE observation, involving the electric quadrupole transition between $D_{5/2}$ and $S_{1/2}$, and using a new "dephasing" measurement protocol based on the STIRAP technique. Other suitable experimental schemes might exist, and we encourage further proposals in this sense.

ACKNOWLEDGMENTS

We thank Siddartha Chattopadhyay and David Wilkowski for helpful discussions. CC acknowledges fruitful discussions with Gonzalo Muga (UPV/EHU). EL would like to thank the Doctoral School "Physique et Sciences de la Matière" (ED 352) for its funding.

Appendix A: Form of the reservoir coupling spectrum for hydrogen-like atoms in free space

Using the notations introduced in Sec. III A, the reservoir coupling spectrum (2) is given by

$$R(\omega) = \sum_{J,M,\lambda} \hbar^{-2} \rho\left(\omega\right) \times \left| \left\langle n_{\mathrm{e}}, l_{\mathrm{e}}, m_{\mathrm{e}}; 0 \right| \hat{H}_I \left| n_{\mathrm{g}}, l_{\mathrm{g}}, m_{\mathrm{g}}; J, M, \lambda, \omega \right\rangle \right|^2. \quad \text{(A1)}$$

Here, the density of states is $\rho\left(\omega\right) = 1$, on account of the normalisation $\left\langle J, M, \lambda, \omega \mid J', M', \lambda', \omega' \right\rangle = \delta_{JJ'}\delta_{MM'}\delta_{\lambda\lambda'}\delta\left(\omega - \omega'\right)$ (this can be understood by dimensional considerations). In the non-relativistic approximation, Seke calculated in [13] the exact matrix elements $\left\langle n_{\mathrm{e}}, l_{\mathrm{e}}, m_{\mathrm{e}}; 0 \right| \hat{H}_I \left| n_{\mathrm{g}}, l_{\mathrm{g}}, m_{\mathrm{g}}; J, M, \lambda, \omega \right\rangle$ for hydrogen-like atoms in free space, using the interaction Hamiltonian (in SI units)

$$\hat{H}_I = \frac{e}{m_e} \hat{\mathbf{A}}\left(\hat{\mathbf{x}}\right) \cdot \hat{\mathbf{p}}\,, \quad \text{(A2)}$$

with e the elementary electric charge, m_e the electron mass, $\hat{\mathbf{x}}$ and $\hat{\mathbf{p}}$ the position and the linear momentum operators of the electron respectively and $\hat{\mathbf{A}}$ the vector potential operator of the quantized EM field. By employing these exact matrix elements (Eqs. (17-19) in [13]) in Eq. (A1), one gets the following analytical form for the reservoir coupling spectrum

$$R(\omega) = \sum_{J,M,\lambda} \hbar^{-1}(-\mathrm{i})^{2J+2\epsilon}\alpha^4 m_e c^3 \times \left\langle l_{\mathrm{g}}, J, m_{\mathrm{g}}, M | l_{\mathrm{g}}, J, l_{\mathrm{e}}, m_e \right\rangle^2 \times \frac{\left(\frac{\omega}{\omega_{\mathrm{X}}}\right)^{2J+2\epsilon-1}}{\left[1+\left(\frac{\omega}{\omega_{\mathrm{X}}}\right)^2\right]^{2(n_{\mathrm{g}}+n_{\mathrm{e}}-1)}} \left(\sum_{r=0}^{N'_J} d'_{Jr}\left(\frac{\omega}{\omega_{\mathrm{X}}}\right)^{2r}\right)^2 \quad \text{(A3)}$$

where c the speed of light in vacuum, α is the fine structure constant of electrodynamics, $\left\langle l_{\mathrm{g}}, J, m_{\mathrm{g}}, M | l_{\mathrm{g}}, J, l_{\mathrm{e}}, m_{\mathrm{e}} \right\rangle$ are the Clebsch-Gordan coefficients of the transition of interest, and ω_{X} is the non-relativistic cutoff frequency given by Eq. (5). The coefficients d'_{Jr} are numerical coefficients that have been calculated for certain transitions in [13] (note that the coefficients d'_{Jr} here correspond to the coefficients $d_{00}d_r$ in Eq. (18) in Ref. [13]). The index at which the sum is terminated is $N'_J = n_{\mathrm{e}} + n_{\mathrm{g}} - 2 - (1/2)(J - l_{\mathrm{e}} - l_{\mathrm{g}} - \epsilon)$ with $\epsilon = 0$ for electric transitions and $\epsilon = 1$ for magnetic transitions. Eq. (A3) can be recast in the form

$$R(\omega) = \sum_{J,M,\lambda} \hbar^{-1}(-\mathrm{i})^{2J+2\epsilon}\alpha^4 m_e c^3 \times \left\langle l_{\mathrm{g}}, J, m_{\mathrm{g}}, M | l_{\mathrm{g}}, J, l_{\mathrm{e}}, m_{\mathrm{e}} \right\rangle^2 \times \sum_{r=0}^{N_J} d_{Jr} \frac{\left(\frac{\omega}{\omega_{\mathrm{X}}}\right)^{2J+2\epsilon-1+2r}}{\left[1+\left(\frac{\omega}{\omega_{\mathrm{X}}}\right)^2\right]^{2(n_{\mathrm{g}}+n_{\mathrm{e}}-1)}} \quad \text{(A4)}$$

where $N_J = 2\left(n_{\mathrm{e}} + n_{\mathrm{g}}\right) - 4 - J - l_{\mathrm{e}} - l_{\mathrm{g}} - \epsilon$ and d_{Jr} are combinations of the previous d'_{Jr} coefficients. Moreover, as a consequence of the conservation of the angular momentum, the values of J and M must verify

$$\begin{cases} J = |l_{\mathrm{e}} - l_{\mathrm{g}}|, |l_{\mathrm{e}} - l_{\mathrm{g}}| + 1, ..., |l_{\mathrm{e}} + l_{\mathrm{g}}| \\ M = m_{\mathrm{e}} - m_{\mathrm{g}} \equiv \overline{M} \end{cases} \quad \text{(A5)}$$

which are the *exact* selection rules. Therefore, the full reservoir takes the form

$$R(\omega) = \sum_{J=|l_{\mathrm{e}}-l_{\mathrm{g}}|}^{|l_{\mathrm{e}}+l_{\mathrm{g}}|} \sum_{M,\lambda} \hbar^{-1}(-\mathrm{i})^{2J+2\epsilon}\alpha^4 m_{\mathrm{e}} c^3 \times \left\langle l_{\mathrm{g}}, J, m_{\mathrm{g}}, M | l_{\mathrm{g}}, J, l_{\mathrm{e}}, m_{\mathrm{e}} \right\rangle^2 \delta_{M\overline{M}} \times \sum_{r=0}^{N_J} d_{Jr} \frac{\left(\frac{\omega}{\omega_{\mathrm{X}}}\right)^{2J+2\epsilon-1+2r}}{\left[1+\left(\frac{\omega}{\omega_{\mathrm{X}}}\right)^2\right]^{2(n_{\mathrm{g}}+n_{\mathrm{e}}-1)}} \quad \text{(A6)}$$

which can be recast in the expression given in the main text by Eq. (4), where we introduced dimensionless coefficients D_{Jr} involving the Clebsch-Gordan coefficients and the other constants and the sums over M and λ.

Appendix B: Derivation of the AZE scaling in the simple case of the reservoir (6)

Here we derive an analytical form of the integral of Eq. (1) with the simplified form of the reservoir (6). Keeping in mind the hierarchy $\omega_0 \ll \omega_{\rm X}$, we will proceed to derive an approximate analytical expression of the general integral

$$I_{\eta\mu}(\tau) = \tau \int_0^{+\infty} \mathrm{d}\omega \, \frac{\omega^\eta}{\left[1+\left(\frac{\omega}{\omega_{\rm X}}\right)^2\right]^\mu} \mathrm{sinc}^2\left((\omega-\omega_0)\frac{\tau}{2}\right) \tag{B1}$$

in terms of which the measurement-modified decay rate (1) is straightforwardly expressed: $\Gamma_\tau = D I_{\eta\mu}(\tau)/\omega_{\rm X}^{\eta-1}$. Using the binomial expansion of ω^η, we first rewrite our integral as

$$I_{\eta\mu}(\tau) = \tau \sum_{k=0}^{\eta} \frac{\eta!}{k!\,(\eta-k)!}\omega_0^{\eta-k} \times \int_0^{+\infty} \mathrm{d}\omega \, \frac{(\omega-\omega_0)^k}{\left[1+\left(\frac{\omega}{\omega_{\rm X}}\right)^2\right]^\mu} \mathrm{sinc}^2\left((\omega-\omega_0)\frac{\tau}{2}\right). \tag{B2}$$

The $k=0$ and $k=1$ terms in the sum may be treated in a specific way. Namely, we make the following approximation of the square cardinal sine function in $F_\tau(\omega)$, that is illustrated in Fig. 1 (b):

$$\mathrm{sinc}^2\left((\omega-\omega_0)\frac{1}{2\nu}\right) \simeq \begin{cases} 1 \text{ for } \omega_0 - \pi\nu < \omega < \omega_0 + \pi\nu\,, \\ 0 \text{ otherwise.} \end{cases} \tag{B3}$$

This approximation is sufficient for $k=0$ and $k=1$ only, as the integrand in (B2) decays sufficiently fast when one moves away from ω_0 so that the frequency ranges outside the door function (B3) can be ignored. In addition to this, in the frequency range of interest here (that is, a small range of width $\sim\nu$ centered on ω_0), we can consider that $\omega/\omega_{\rm X} \sim 0$ (which is justified by the hierarchy $\omega_0 \ll \omega_{\rm X}$). Using these approximations, we can write the low-k contribution to the integral as

$$\begin{aligned} &\tau \sum_{k=0}^{1} \frac{\eta!}{k!\,(\eta-k)!}\omega_0^{\eta-k} \\ &\quad\times \int_0^{+\infty} \mathrm{d}\omega \, \frac{(\omega-\omega_0)^k}{\left[1+\left(\frac{\omega}{\omega_{\rm X}}\right)^2\right]^\mu} \mathrm{sinc}^2\left((\omega-\omega_0)\frac{\tau}{2}\right) \\ &\quad\simeq \tau \sum_{k=0}^{1} \frac{\eta!}{k!\,(\eta-k)!}\omega_0^{\eta-k} \int_{\omega_0-\pi\nu}^{\omega_0+\pi\nu} \mathrm{d}\omega \, (\omega-\omega_0)^k \\ &\quad= 2\pi\,\omega_0^\eta. \end{aligned} \tag{B4}$$

Now we turn to the terms for which $k \geq 2$ and that will only exist if $\eta > 1$. For these terms, replacing the square cardinal sine by a rectangle function is no longer valid, as the growth of $(\omega-\omega_0)^k$ is not overridden by the decrease of $(\omega-\omega_0)^{-2}$ that comes from the square cardinal sine, and therefore we must consider the whole frequency range. We therefore need to find another way to approximate the integral (B2), and we may simply replace the square sine by its mean value $1/2$ here to get

$$\mathrm{sinc}^2\left((\omega-\omega_0)\frac{1}{2\nu}\right) \simeq \frac{2\nu^2}{(\omega-\omega_0)^2}. \tag{B5}$$

Also note, that we should not have ω_0/ν excessively large, lest the square cardinal sine converges to the Dirac δ distribution, and replacing the square sine with its average value is no longer valid. We then compute the resulting integral, which, in the limit $\omega_0/\omega_{\rm X} \to 0$, acceptable for the transitions that interest us, reads

$$\begin{aligned} &\int_0^{+\infty} \mathrm{d}\omega \, \frac{(\omega-\omega_0)^{k-2}}{\left[1+\left(\frac{\omega}{\omega_{\rm X}}\right)^2\right]^\mu} \\ &\qquad\simeq \frac{1}{2}\omega_{\rm X}^{k-1} B\left(\frac{1-k}{2}+\mu, -\frac{1-k}{2}\right) \end{aligned} \tag{B6}$$

where B refers to Euler's Beta function. As can be checked from (B2) and (B6), of all the contributions for $k \geq 2$, the one for which $k=\eta$ is easily the largest (this is due, again, to the hierarchy $\omega_0 \ll \omega_{\rm X}$). As such, we can rewrite (B2) as

$$I_{\eta\mu}(t) \simeq 2\pi\,\omega_0^\eta + \nu\,\omega_{\rm X}^{\eta-1} B\left(\frac{1-\eta}{2}+\mu, -\frac{1-\eta}{2}\right) \tag{B7}$$

where the second summand on the r.h.s. of (B7) will only exist for $\eta > 1$. Comparison with the natural decay rate $\Gamma_0 = 2\pi R(\omega_0) \simeq 2\pi D\omega_0^\eta/\omega_{\rm X}^{\eta-1}$ (as $\omega_0 \ll \omega_{\rm X}$) yields

$$\begin{aligned} \frac{\Gamma_\tau}{\Gamma_0} &\simeq 1 + \frac{1}{2\pi}\frac{\nu}{\omega_0} \\ &\qquad\times \left(\frac{\omega_{\rm X}}{\omega_0}\right)^{\eta-1} B\left(\frac{1-\eta}{2}+\mu, -\frac{1-\eta}{2}\right). \end{aligned} \tag{B8}$$

Note that this result had been (partially) obtained in [1], where the authors found that for a reservoir of the form $R(\omega) \propto \omega^\eta$ with $\eta > 1$: $\Gamma \propto \nu\,\omega_{\rm X}^{\eta-1}$, in the approximation $\omega_0^\eta/\omega_{\rm X}^{\eta-1} \ll \nu \ll \omega_{\rm X}$ (*cf.* Eq. (20) in Ref. [1]).

Appendix C: Derivation of the AZE scaling in the complete case of the reservoir (4)

In this section, we extend the previous result found for a reservoir of the simple form (6) to the general form (4). Let us first sum over r, and then over J. In the generic case, the FGR decay rate will be, for the reservoir coupling spectrum (4), given by

$$\Gamma_{0J} = D_{J0} 2\pi \frac{\omega_0^{\eta_J}}{\omega_{\rm X}^{\eta_J-1}}. \tag{C1}$$

This is true unless D_{J0} vanishes. This is the case for instance of the electric dipole transitions ($\epsilon = 0$, $J = 1$) between levels sharing the same principal quantum number (see Table I in Ref. [13]), due to the special properties of these dipolar transitions. That D_{J0} vanishes can be shown rather easily by using the orthogonality properties of the Gegenbauer polynomials (see Ref. [29] for a derivation of the momentum-space wave functions of hydrogen in terms of these polynomials). However, we do not focus on this special case here. In the generic case ($D_{J0} \neq 0$), the decay rate under frequent observations for a specific J will be

$$\Gamma_{\tau J} \simeq 2\pi\, D_{J0}\, \frac{\omega_0^{\eta_J}}{\omega_{\rm X}^{\eta_J-1}} + \nu \times \sum_{r=0}^{N_J} D_{Jr}\, \theta\left(\eta_J + 2r - \frac{3}{2}\right) \times\, B\left(\frac{1-\eta_J-2r}{2}+\mu, -\frac{1-\eta_J-2r}{2}\right). \quad \text{(C2)}$$

with θ the Heaviside step function. It thus appears that, for given J, all terms in the sum over r in (4) have a contribution to the modified decay rate that is of the same order of magnitude. All that remains to be done is to sum over J. This sum is resolved quite differently for the free decay rate on the one hand, and the modified decay rate on the other. Namely, for the former, we see from (C1) that the hierarchy $\omega_0 \ll \omega_{\rm X}$ ensures that the contribution from the smallest possible J is dominant. This value is equal to $|l_{\rm e} - l_{\rm g}| \equiv J_{\rm min}$, and we will write $\eta_{\rm min} \equiv \eta_{J_{\rm min}}$. For the latter, however, we are forced to keep the double sum over J and N_J: all (sufficiently large) powers of the frequency in the coupling contribute to the modified decay rate on the same level, with numerical prefactors as the sole difference. Namely, writing $\Gamma_0 = \sum_{J=|l_{\rm e}-l_{\rm g}|}^{l_{\rm e}+l_{\rm g}} \Gamma_{0J}$ and $\Gamma_\tau = \sum_{J=|l_{\rm e}-l_{\rm g}|}^{l_{\rm e}+l_{\rm g}} \Gamma_{\tau J}$, we have obtained

$$\frac{\Gamma_\tau}{\Gamma_0} \simeq 1 + \frac{1}{2\pi}\frac{\nu}{\omega_0}\left(\frac{\omega_{\rm X}}{\omega_0}\right)^{\eta_{\rm min}-1} \sum_{J=|l_{\rm e}-l_{\rm g}|}^{l_{\rm e}+l_{\rm g}} \sum_{r=r_0}^{N_J} \frac{D_{Jr}}{D_{J_{\rm min}0}} \times B\left(\frac{1-\eta_J-2r}{2}+\mu, -\frac{1-\eta_J-2r}{2}\right) \quad \text{(C3)}$$

where we have introduced

$$r_0 \equiv \max\left\{\left\lfloor \frac{3}{4} - \frac{\eta_J}{2} \right\rfloor, 0\right\}. \quad \text{(C4)}$$

Despite the more complicated appearance of this expression, we see that the parametric dependence of the ratio of the decay rates is independent of the details of the matrix elements: the important parameter is $\eta_{\rm min}-1$. There is a competition between $\nu/\omega_0 \ll 1$ and $\omega_{\rm X}/\omega_0 \gg 1$ but, for $\eta_{\rm min} \geq 3$, we can expect that the second factor will dominate, especially for low values of Z [see Eq. (7)]. This second factor becomes all the more dominant for higher values of $\eta_{\rm min}$, that is, for transitions with high difference between the orbital angular momenta of the initial and final levels. Only for transitions where $|l_{\rm e} - l_{\rm g}| = 1$ does the second factor $(\omega_{\rm X}/\omega_0)^0 = 1$ fail to play a role, so that they verify $\Gamma_\tau \simeq \Gamma_0$. These transitions are often called "electric dipole transitions" (including by us in our Sec. I), although in most cases they are accompanied by emission of photons of angular momentum $J > 1$ (as well of course as $J = 1$). Indeed, as we have recalled with Eq. (C1), it is always the photons with the smallest allowed value $J_{\rm min}$ of J that dominate the *spontaneous* emission in an electronic transition.

[1] A. G. Kofman and G. Kurizki, Nature **405**, 546 (2000).
[2] P. Facchi, H. Nakazato, and S. Pascazio, Phys. Rev. Lett. **86**, 2699 (2001).
[3] B. Misra and E. C. G. Sudarshan, J. Math. Phys. **18**, 756 (1977).
[4] R. Cook, Phys. Scr. **1988**, 49 (1988).
[5] W. M. Itano, D. J. Heinzen, J. J. Bollinger, and D. J. Wineland, Phys. Rev. A **41**, 2295 (1990).
[6] Y. S. Patil, S. Chakram, and M. Vengalattore, Phys. Rev. Lett. **115**, 140402 (2015).
[7] B. Kaulakys and V. Gontis, Phys. Rev. A **56**, 1131 (1997).
[8] A. G. Kofman and G. Kurizki, Phys. Rev. A **54**, R3750 (1996).
[9] M. Lewenstein and K. Rzażewski, Phys. Rev. A **61**, 022105 (2000).
[10] M. C. Fischer, B. Gutiérrez-Medina, and M. G. Raizen, Phys. Rev. Lett. **87**, 040402 (2001).
[11] P. M. Harrington, J. T. Monroe, and K. W. Murch, Phys. Rev. Lett. **118**, 240401 (2017).
[12] H. Moses, Phys. Rev. A **8**, 1710 (1973).
[13] J. Seke, Phys. A **203**, 269 (1994).
[14] C. Cohen-Tannoudji, J. Dupont-Roc, and G. Grynberg, *Photons and atoms: introduction to quantum electrodynamics* (Wiley Online Library, 1989).
[15] H. Zheng, S. Y. Zhu, and M. S. Zubairy, Phys. Rev. Lett. **101**, 200404 (2008).
[16] Q. Ai, Y. Li, H. Zheng, and C. P. Sun, Phys. Rev. A **81**, 042116 (2010).
[17] Z. Zhou, Z. Lü, H. Zheng, and H.-S. Goan, Phys. Rev. A **96**, 032101 (2017).
[18] A. Z. Chaudhry, Sci. Rep. **6**, 29597 (2016).
[19] P. Facchi and S. Pascazio, Phys. Lett. A **241**, 139 (1998).
[20] V. Debierre, T. Durt, A. Nicolet, and F. Zolla, Phys. Lett. A **379**, 2577 (2015).
[21] M. S. Safronova, W. R. Johnson, and U. I. Safronova, Journal of Physics B: Atomic, Molecular and Optical Physics **43**, 074014 (2010).
[22] M. S. Safronova, W. R. Johnson, and U. I. Safronova, Journal of Physics B: Atomic, Molecular and Optical Physics **50**, 189501 (2017).
[23] A. G. Kofman and G. Kurizki, Phys. Rev. Lett. **87**, 270405 (2001).
[24] Q. Ai, D. Xu, S. Yi, A. G. Kofman, C. P. Sun, and F. Nori, Sci. Rep. **3** (2013).

[25] J. R. Kuklinski, U. Gaubatz, F. T. Hioe, and K. Bergmann, Phys. Rev. A **40**, 6741 (1989).
[26] J. L. Sørensen, D. Møller, T. Iversen, J. B. Thomsen, F. Jensen, P. Staanum, D. Voigt, and M. Drewsen, New J. Phys. **8**, 261 (2006).
[27] H. Dehmelt, in *Bull. Am. Phys. Soc.*, Vol. 20 (1975) p. 60.
[28] A. Kreuter, C. Becher, G. P. T. Lancaster, A. B. Mundt, C. Russo, H. Häffner, C. Roos, W. Hänsel, F. Schmidt-Kaler, R. Blatt, and M. S. Safronova, Phys. Rev. A **71**, 032504 (2005).
[29] B. Podolsky and L. Pauling, Phys. Rev. **34**, 109 (1929).